Constraining R-parity-violating couplings in τ -processes at the LHC and in electroweak precision measurements

Saurabh Bansal[®], Antonio Delgado, Christopher Kolda, and Mariano Quiros^{1,2} ¹Department of Physics, University of Notre Dame, 225 Nieuwland Hall, Notre Dame, Indiana 46556, USA ²Institut de Física d'Altes Energies (IFAE) and BIST, Campus UAB 08193, Bellaterra, Barcelona, Spain

(Received 5 August 2019; published 22 November 2019)

We find new limits on the nine λ'_{3ik} R-parity violating couplings of the minimal supersymmetric standard model, using Drell-Yan differential cross sections at the LHC and electroweak precision measurements from LEP and SLC. Specifically, limits on six of the nine λ'_{3jk} -couplings, with j=1 or 2, are obtained using Drell-Yan data, providing the strongest bounds on three of these couplings. Four of the nine couplings are currently best constrained by electroweak data, which we reexamine here using a specifically lepton flavor-violating observable. The remaining two couplings are best constrained due to their contributions to neutrino masses, a bound which we update here. We also update previous limits on all λ'_{ijk} -couplings using both electroweak data and neutrino mass bounds. A table of all current bounds on λ'_{ijk} is given in the Appendix.

DOI: 10.1103/PhysRevD.100.093005

I. INTRODUCTION

With the discovery of the Higgs boson and the completion of the Standard Model (SM) particle spectrum, the search for physics beyond the Standard Model (BSM) is well underway. Among the wide range of possible BSM models, supersymmetry (SUSY) offers a particularly attractive alternative, providing a solution to the hierarchy problem and offering a robust framework for approaching many of the other problems of the SM. But while SUSY may have some very strong theoretical motivations, experiments have yet to find signatures of the most minimal SUSY model in its expected parameter space. This has led physicists to explore less minimal versions of SUSY, including its R-parity violating version.

R-parity was originally imposed on the minimal supersymmetric standard model (MSSM) in an attempt to avoid problems with fast proton decay; as a side effect, it generated an attractive dark matter candidate in the form of the lightest (necessarily stable) SUSY particle (LSP). But the presence of R-parity (or lack thereof) also plays a key role in determining how one should search for the presence of SUSY at colliders such as the LHC. In particular, models with unbroken R-parity always pair-produce SUSY

Published by the American Physical Society under the terms of the Creative Commons Attribution 4.0 International license. Further distribution of this work must maintain attribution to the author(s) and the published article's title, journal citation, and DOI. Funded by SCOAP³.

particles and leave missing energy signatures as the SUSY particles decay down to the LSPs, which escape the detector unseen. Most of the key strategies for studying SUSY at colliders involve this particular production path: on-shell pair production, leading to missing energy in the detector. In turn, very strong bounds have been placed on the majority of SUSY particles, constraining their masses to be generally above 500 GeV to 2 TeV [1].

In SUSY models with R-parity violation (RPV), the above search strategy generally fails, though other search avenues open up that can help fill the breach. In a previous work (Ref. [2]), we studied a technique for placing strong constraints on the parameter space from the study of Drell-Yan (DY) processes (both neutral and charged current) at the LHC. In models with RPV, SUSY partners can be exchanged by SM particles at tree level, something that is not possible in R-parity conserving models, leading to sizable interference effects in SM processes. In Ref. [2], we analyzed the effect of an RPV coupling λ'_{ijk} (there are 27 such couplings, defined in the next section) on DY processes involving electrons and muons final states. We found that the LHC could already place surprisingly strong constraints in wide regions of the parameter space of squark masses and λ'_{iik} , for couplings to the first- and second-generation leptons.

In this paper we return to this subject and work to place bounds for the case in which the only available RPV coupling is to τ -leptons using the same techniques. In addition, we revisit precision electroweak constraints on RPV, mostly derived from the LEP and SLC data, to show that the current best fits place stronger constraints on certain λ'_{ijk} couplings than previously advertised. In all, we present new bounds on 11 of the 27 λ'_{ijk} couplings, all of which are stronger than existing bounds found in the literature. Last, we reexamine constraints coming from bounds on neutrino masses, which provide extremely strong constraints on six of the 27 couplings; these bounds have appeared in the literature before, but we recast them here in a more useful form.

The paper is organized as follows: in Sec. II we introduce the model and processes that will be studied; we then present the analysis and results for Drell-Yan processes in Sec. III and electroweak processes in Sec. IV. In Sec. V, we discuss and update bounds due to neutrino masses. Finally, we devote Sec. VI to our conclusions. For completeness, we summarize in Appendix the current bounds on all the $27 \ \lambda'_{iik}$ couplings.

II. L-VIOLATING RPV

R-parity is a multiplicative quantum number, defined as

$$R_P = (-1)^{3(B-L)+2s},\tag{1}$$

where B is the baryon number, L the lepton number, and s is the spin of a specific state. R-parity is usually enforced in the MSSM and allows, as the most general superpotential,

$$\mathcal{W}_{R_P} = Y_{ij}^u U_i^c Q_j H_u - Y_{ij}^d D_i^c Q_j H_d$$
$$- Y_{ij}^e E_i^c L_j H_d + \mu H_u H_d,$$

where H_u and H_d are two Higgs doublets with hypercharges $\pm 1/2$, respectively. Here, L and Q are the SU(2) doublets, while E^c , D^c , and U^c are singlets, and Y^U_{ij} , Y^D_{ij} , and Y^E_{ij} the Yukawa coupling matrices. The above superpotential prevents tree-level processes where B and/or L are violated and has strong phenomenological implications, including the fact that supersymmetric partners should be pair produced in colliders and that the LSP is stable and can become a dark matter candidate. However, in view of the strong experimental bounds on theories with R-parity conservation, one can extend the above superpotential by including R-parity-breaking terms, which soften the present experimental bounds.

In the MSSM, the RPV portion of the trilinear superpotential can be written as

$$\mathcal{W}_{\not I_P} = rac{1}{2} \lambda_{ijk} L_i L_j E_k^c + \lambda'_{ijk} L_i Q_j D_k^c + rac{1}{2} \lambda''_{ijk} U_i^c D_j^c D_k^c.$$

Using the standard notation, we have defined λ_{ijk} , λ'_{ijk} , and λ''_{ijk} as new Yukawa couplings, where i, j, and k are the generation indices; we omit a bilinear term that mixes sleptons and Higgs fields. In order to enforce B-conservation, we assume the λ''_{ijk} are all zero, but λ_{ijk} and λ'_{ijk} remain. Moreover, for the purpose of this work, we will only concentrate on the λ'_{ijk} interactions. Furthermore, as we did in Ref. [2], we will only take one element of λ'_{ijk} at a time to

be nonzero, in order to avoid the (possibly) complicated interference effects, and the potentially large contributions to quark or lepton flavor-changing amplitudes.

As we mentioned above, in Ref. [2], the constraints from Drell-Yan processes on λ'_{ijk} couplings involving electrons and muons, i.e., i=1 and 2, were studied. In this paper, we will concentrate on λ'_{ijk} couplings involving taus, i.e., i=3. In this scenario, the RPV superpotential leads to the following Lagrangian in the up-quark mass basis:

$$\mathcal{L} = \lambda'_{3jk} [((V\bar{d}^c)_j P_L \nu_\tau - \bar{u}_j^c P_L \tau) \tilde{d}_{Rk}^* + (\bar{d}_k P_L \nu_\tau (V\tilde{d}_L)_j - \bar{d}_k P_L \tau \tilde{u}_{Lj}) + (\bar{d}_k P_L (Vd)_j \tilde{\nu}_{\tau L} + \bar{d}_k P_L u_j \tilde{\tau}_L)] + \text{H.c.}$$
(2)

Here *V* is the Cabibbo–Kobayashi–Maskawa (CKM) matrix, which we will consider in the (reasonable for our purposes) diagonal approximation.

One of the key points to notice is that the λ'_{ijk} couplings cause the squarks to couple as scalar leptoquarks; that is, they interact with both quarks and leptons at a single vertex. As such, squarks can be exchanged in the *t*-channel in DY scattering and can appear in loops in Z-decay, two processes that we will consider in the following two sections.

In the next two sections, we present our analysis and results for Drell-Yan and electroweak processes, separately.

III. CONSTRAINTS FROM DRELL-YAN PROCESSES

The contributions of scalar leptoquarks to DY scattering processes were recently studied in both the neutral current channel [3,4] and the charged current channel [5]. As with these previous papers, we will refer to the neutral current case as dilepton DY scattering, since the final state is always $\ell^+\ell^-$ with both leptons of the same flavor (assuming only a single RPV coupling at a time), and the charged current as monolepton DY scattering, since the final state is of the form $\ell\nu_\ell$. In Ref. [2], we specialized this analysis to RPV SUSY, studying the $\lambda'_{ijk}L_iQ_jD_k^c$ superpotential coupling, for i=1 (final state electrons) and i=2 (final state muons). In both of these final states, excellent analyses of DY data had been completed by both ATLAS and CMS at $\sqrt{s}=13$ TeV. (See Ref. [6] for a similar analysis using Tevatron dilepton data.)

The situation for final state τ -leptons is not as simple at present. DY mono-tau searches have been published by both ATLAS [7] and CMS [8] over a wide range of transverse mass. But a similar search for the di-tau process is not available from either of the collaborations. There is a measurement of di-taus from the CMS Collaboration [9], but it is limited to small invariant masses ($m_{\tau\tau} < 250$ GeV) and low integrated luminosity (2.3 fb⁻¹). The low invariant mass range studied, and the large statistical errors, will prevent us from placing strong constraints using that dataset. Due to these limitations, we will only be able to use the

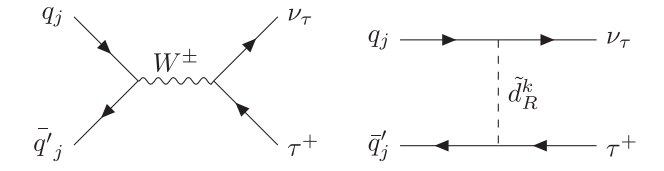


FIG. 1. Feynman diagrams for mono-tau production in the SM (left) and supersymmetry with RPV (right).

mono-tau DY process to constrain the RPV couplings involving τ -leptons.

The λ'_{ijk} couplings contribute to the mono-tau process due to the first two terms in Eq. (2) involving \tilde{d}_R^k . After integrating out \tilde{d}_R^k , these terms generate the operator $(\bar{\nu}_{\tau}P_Rd_g^c)(\bar{u}_j^cP_L\tau)$, which, after fierzing, equals (1/2) $(\bar{d}_j\gamma^{\mu}P_Lu_j)(\bar{\nu}_{\tau}\gamma_{\mu}P_L\tau)$. Thus, this operator directly interferes with the SM process. The Feynman diagrams for this process in the SM and RPV SUSY are shown in Fig. 1, with the latter contributing through a \tilde{d}_R^k -mediated t-channel process with d_j and u_j in the initial state. Note that after integrating out \tilde{d}_R^k , the contribution from RPV SUSY only depends on the value of j. In other words, for a fixed value of j, the constraints on λ'_{3jk} are the same for all k.

Since quarks in the initial state at LHC have differing parton distribution functions (PDFs), the constraints on λ'_{3jk} strongly depend on the value of j. The constraints are strongest for j=1, due to the large PDFs of u- and d-quarks, followed by somewhat weaker constraints for j=2, weaker mostly because of the suppressed PDFs of c-quarks. But since the PDF of the top quark can be taken to be zero, λ'_{3jk} with j=3 is not constrained at all. In total, the mono-tau analysis using LHC data can be used to constrain six out of ten λ'_{3jk} couplings.

We now provide a brief overview of our analysis for Drell-Yan processes, and we refer the interested reader to Ref. [2] for a more detailed account. The analysis done here is similar to that of Ref. [2], with final state electrons and muons replaced by taus. As mentioned above, due to the lack of a di-tau search at the LHC in the right kinematic regime and with sufficient luminosity, we will not be able to use di-tau data to constrain our parameter space. But when the required analysis has been performed by ATLAS and/or CMS, the work done here can be replicated for di-tau processes as well, though a preferable option would be for the collaborations to complete their own interpretation of DY data in terms of bounds on RPV SUSY couplings, following the model here and in Ref. [2].

As discussed above, the mono-tau DY bounds on λ'_{3jk} are independent of k; that is, the squark mass bounds we obtain are the same for each of the \tilde{d}^k_R squarks, for k=1,2,3. And since we always take i=3 (final state as τ -leptons), the only remaining dependence is on j. For each value of j, we calculate the constraints in the $m_{\tilde{d}^k_R}$ versus λ'_{3ik} plane, by comparing the RPV prediction to the

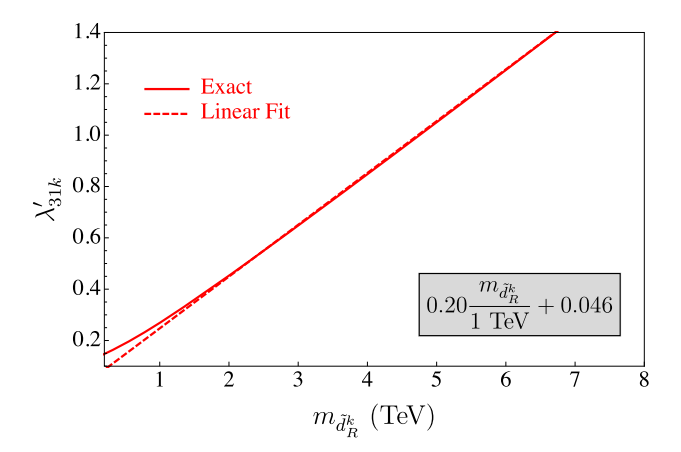


FIG. 2. The 95% C.L. upper bound (solid line) on λ'_{31k} using monolepton data. A linear fit (dashed line) to this bound and the corresponding equation are also shown.

experimental measurements. These measurements are published by both ATLAS [7] and CMS [8] Collaborations at $\sqrt{s} = 13$ TeV with 36 fb⁻¹ of integrated luminosity. In this work, we compare with the ATLAS data as they are readily available at https://www.hepdata.net. The signal events are obtained by simultaneously calculating the SM plus RPV contribution to the transverse mass (m_T) spectrum for $pp \to \tau \nu_{\tau}$ processes. These calculations are done analytically at the leading order, using the MSTW 2008 next-tonext-to leading order (NNLO) PDFs [10]. The resulting spectrum is then rescaled bin by bin to account for the higherorder corrections and lepton reconstruction efficiency, so that our SM ("background") spectrum matches the irreducible background data from ATLAS. Finally, the net signal plus background is obtained by adding the reducible background to the generated event distribution.

To quantify the effect of our signal, and to estimate the limits on the RPV parameters, we use a conservative version of a $\Delta \chi^2$ test. Specifically, 95% C.L. limits are obtained when $\Delta \chi^2 \equiv \chi^2_{\rm model} - \chi^2_{\rm SM} = 5.99$. The systematic errors used in this test are taken, bin by bin, from the ATLAS searches [7], which range from about 15% at low transverse masses (~200 GeV) to over 50% at high transverse masses. Finally, we quote our limits on the model by fitting a straight line in the $(m_{\tilde{d}_R^k}, \lambda'_{3jk})$ -plane to the 95% C.L. contour in the region where $m_{\tilde{d}_R^k} \geq 1$ TeV. Below 1 TeV squark masses, the constraints are far less linear, and the squarks themselves are often better constrained by direct production limits. Thus, the limits we quote only hold for $m_{\tilde{d}_p^k} > 1$ TeV. The accuracy of our linear fit can be seen in Fig. 2, where the 95% C.L. contour (solid line) and a linear fit (dashed line) to this contour are shown for λ'_{31k} .

Our resulting constraints from monolepton DY processes are summarized in the second column of Table I. The first column indicates the existing bound in the literature, collected and updated in Refs. [11–17]. These bounds

32k

33k

Sec. V. $\frac{ijk}{1.11 \frac{m_{\tilde{d}_k}}{1 \text{ TeV}}} \qquad 0.20 \frac{m_{\tilde{d}_k}}{1 \text{ TeV}} + 0.046 \qquad 1.5 \frac{m_{\tilde{t}}}{1 \text{ TeV}} + 0.41 \qquad 0.14 \frac{m_{\tilde{d}_k}}{1 \text{ TeV}} + 0.046$

TABLE I. Upper bounds on λ'_{3jk} (k = 1, 2, 3) from the literature and derived in this study. Projected bounds are obtained using a mono-tau analysis assuming 3 ab⁻¹ of data. For bounds from neutrino mass contributions, see Sec. V.

are derived from $R_{\tau\pi} = \Gamma(\tau \to \pi\nu_{\tau})/\Gamma(\mu \to \pi\nu_{\mu})$ for λ'_{31k} ; $R_{D_s} = \Gamma(D_s \to \tau\nu_{\tau})/\Gamma(D_s \to \mu\nu_{\mu})$ for λ'_{32k} ; and $R_{\tau} = \Gamma(Z \to \text{had})/\Gamma(Z \to \tau\bar{\tau})$ for λ'_{33k} . The constraints on λ'_{33k} are discussed in more detail below.

 1.24^{a}

One must note that the current ATLAS mono-tau data show a small *excess* over the SM predictions for most of the m_T -bins. On the other hand, the RPV monolepton operator interferes *destructively* with the SM, pulling down the expected cross section. Thus the resulting constraints on λ'_{3jk} are much stronger than one would expect just by comparing to the SM distribution. This same excess of events in the data also results in a constraint on λ'_{32k} that is surprisingly strong despite being suppressed by the c-quark PDF. Thus one should keep in mind that if the mono-tau data were to become more closely aligned with the SM prediction, the bounds would weaken. Similar observations were also made for mono-muons in Ref. [2].

Unsurprisingly, the limits we obtain are very sensitive to current experimental uncertainties in the DY spectrum, and so these limits may strengthen or weaken with higher integrated luminosity, at least at first. But we can also make a simple projection of the expected limits on $\{m_{\tilde{q}}, \lambda'_{ijk}\}$ at the high luminosity LHC with 3 ab⁻¹ of integrated luminosity and $\sqrt{s}=13$ TeV, assuming the data matches the SM predictions. In this analysis, we again use the transverse mass dependent systematic error as seen across bins in the current ATLAS data and neglect all sources of reducible background. The last column of Table I indicates these expected limits from a 3 ab⁻¹ high luminosity LHC.

As expected, the constraints obtained from the LHC monolepton analysis are strongest when the quarks involved are first generation, and they weaken significantly when one requires second generation quarks in the initial state (by roughly a factor of 10 in going from λ'_{31k} to λ'_{32k}). In such a case, the dilepton bound would be expected to outdo the monolepton bound, which is another reason why the absence of an experimental DY dilepton analysis hampers the setting of the strongest possible bounds right now. For λ'_{33k} , monolepton searches at the LHC are completely insensitive and another route must be sought in order to obtain bounds on this coupling; we discuss this case in the next section.

IV. ELECTROWEAK CONSTRAINTS

 $1.5 \frac{m_{\tilde{f}}}{1 \text{ TeV}} + 0.41$

 $0.54 \frac{m_{\tilde{f}}}{1 \text{ TeV}} + 0.38$

LHC bounds on the λ'_{33k} couplings are nonexistent currently and will be weak, at best, in the future (using dilepton data, once available). Luckily, there is a wellknown auxiliary bound that can be placed on all of the RPV couplings coming from precision electroweak observables. In particular, the RPV couplings can affect electroweak observables at one loop by modifying the coupling strength of Z to fermions. Since these observables have been measured very precisely by both LEP and SLC at, and above, the Z-pole, the λ'_{ijk} couplings can be constrained by quantifying these modifications. This requires the calculation of RPV-induced $Z \rightarrow f\bar{f}$ one-loop diagrams, shown in Fig. 3, where f is any of ℓ_i , ν_i , u_j , d_j , and d_k for a nonzero λ'_{iik} . Each final state f can have multiple different fermions and sfermions in the loop; for example, a nonzero λ'_{332} can lead to $Z \to \tau \bar{\tau}$ with a t_L -quark and \tilde{s}_R as well as a s_R -quark and \tilde{t}_L in the loop. By calculating all the possible one-loop diagrams for a single nonzero λ'_{ijk} , the RPV parameter space is constrained.

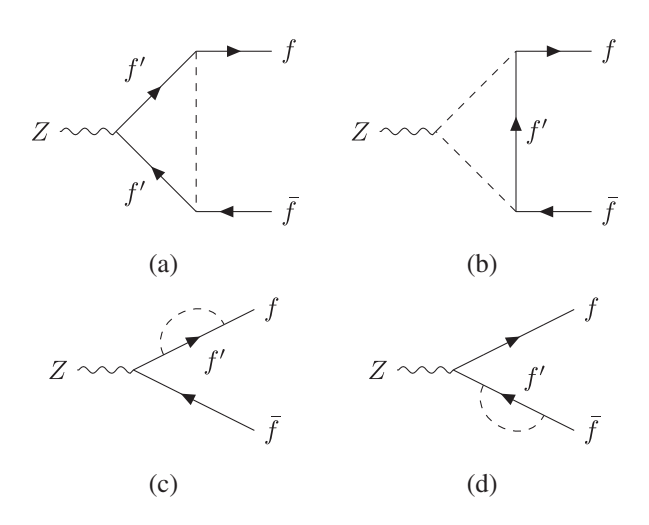


FIG. 3. Feynman diagrams for $Z \to f\bar{f}$ via RPV couplings. The dashed lines represent the exchange of the scalars S and/or \tilde{S} defined in the text.

^aSee text for an explanation of this bound which holds for sfermion masses of 1 TeV.

One may expect that the effect of one-loop diagrams with $\mathcal{O}(\text{TeV})$ sfermion masses would be negligible at the Z-pole. But it has long been known (e.g., [18–20]) that the contribution of these diagrams with t-quarks in the loop can be fairly large. This is the result of helicity flips on the t-quark lines. Since the λ'_{ijk} couplings can contribute a t-quark for j = 3, we expect relatively strong electroweak constraints on λ'_{i3k} . In this section, we will analyze the contributions of RPV to precision electroweak observables in order to constrain the set of couplings λ'_{i3k} . We are hardly the first to do this analysis; previous analyses were performed by Refs. [13,21–25]. Our analysis uses updated electroweak parameters (mostly updated SM predictions for the precision electroweak observables) that have the effect of strengthening the bounds somewhat. But we will also be using an alternative observable, defined below, that allows for an improvement on the electroweak constraints on λ'_{33k} of roughly 25% for sfermion masses of 1 TeV. As a cross-check, we also performed our fits using the observables, data, and SM fits of previous authors, and successfully reproduced the previously obtained bounds.

Before specializing to the problem at hand, we first stop to consider a somewhat more general calculation. Consider a toy model with two scalars, S and \tilde{S} , which interact with the fermions of the SM through the Lagrangian:

$$\mathcal{L} = \sum_{X=L,R} \{ \lambda_X S \overline{f'^c} f_X + \tilde{\lambda}_X \tilde{S} \, \bar{f'} f_X + \text{H.c.} \}.$$
 (3)

Here $f_{L,R}$ and $f'_{L,R}$ are chiral SM states with their usual gauge quantum numbers, while the quantum numbers of S and \tilde{S} are chosen such that the terms in the Lagrangian are gauge invariant. These scalars can then modify the $Z \to \bar{f}f$ amplitude through the Feynman diagrams shown in Fig. 3, with f' being the loop fermion. Since there is a discontinuity in the amplitude of the first diagram [Fig. 3(a)] at $m_{f'} = m_Z/2$, the contributions from these diagrams can be divided into two cases: for $m_{f'} \simeq 0$ and $m_{f'} > m_Z/2$. All the fermions of the SM fall into the first category except for the t-quark, which clearly belongs to the second case. Meanwhile, we assume the common mass of all scalars, denoted by M, to be much greater than m_Z , and thus there is no discontinuity in the second diagram [Fig. 3(b)].

We can absorb the contributions from the one-loop diagrams into a redefinition of the $Z\bar{f}f$ couplings, via

$$\mathcal{L}_{Z} = \frac{g_2}{c_w} \sum_{X = I, P} (g_X^f + \Delta g_X^f) Z_{\mu} \bar{f}_X \gamma^{\mu} f_X, \tag{4}$$

where $g_L^f = T_3^f - Q^f s_w^2$, $g_R^f = -Q^f s_w^2$, and T_3^f is the weak T_3 of the left-handed fermion f_L . The leading order corrections to the $Z\bar{f}f$ couplings due to S, taken from Appendix B of Ref. [20], can be written as follows:

Case I: $m_{f'} \sim 0$:

$$\Delta g_{L/R}^{f} = \frac{|\lambda_{L/R}|^{2} m_{Z}^{2} N_{c}^{f'}}{288 \pi^{2} M^{2} N_{c}^{f}} \times \left\{ g_{L/R}^{f} - g_{L/R}^{f'} \left(12 \log \frac{M}{m_{Z}} + 1 + i6\pi \right) \right\}.$$
(5)

Case II: $m_{f'} > m_Z/2$:

$$\begin{split} \Delta g_{L/R}^f &= \pm \frac{|\lambda_{L/R}|^2 m_{f'}^2 T_3^{f'} N_c^{f'}}{16 \pi^2 M^2 N_c^f} \left(2 \log \frac{M}{m_{f'}} - 1 \right) \\ &+ \frac{|\lambda_{L/R}|^2 m_Z^2 N_c^{f'}}{288 \pi^2 M^2 N_c^f} \\ &\times \left\{ g_{L/R}^f - g_{L/R}^{f'} \left(12 \log \frac{M}{m_{f'}} - 9 \right) \pm 3 T_3^{f'} \right\}, \end{split}$$

where M is the mass of S, and $N_c^{f,f'}$ is the color factor of the final fermion state, f, or of the internal loop fermion, f' (i.e., 3 for a color triplet, 1 for a singlet). The imaginary piece that arises in Case I is due to the loop fermions going on shell, but does not contribute to Z-pole observables. Also note that the $\pm 3T_3^{f'}$ term at the end of Eq. (6) corrects a typographical error in Ref. [20].

Similarly, on computing the amplitudes involving \tilde{S} , we find the dominant parts of the corrections to $Z\bar{f}f$ couplings for the two cases to be the following:

Case I: $m_{f'} \sim 0$:

$$\Delta g_{L/R}^{f} = \frac{|\tilde{\lambda}_{L/R}|^{2} m_{Z}^{2} N_{c}^{f'}}{288 \pi^{2} M^{2} N_{c}^{f}} \times \left\{ g_{L/R}^{f} + g_{R/L}^{f'} \left(12 \log \frac{M}{m_{Z}} + 1 + \mathbf{i} 6\pi \right) \right\}.$$
(7)

Case II: $m_{f'} > m_Z/2$:

$$\begin{split} \Delta g_{L/R}^f &= \pm \frac{|\tilde{\lambda}_{L/R}|^2 m_{f'}^2 T_3^{f'} N_c^{f'}}{16 \pi^2 M^2 N_c^f} \left(2 \log \frac{M}{m_{f'}} - 1 \right) \\ &+ \frac{|\tilde{\lambda}_{L/R}|^2 m_Z^2 N_c^{f'}}{288 \pi^2 M^2 N_c^f} \\ &\times \left\{ g_{L/R}^f + g_{R/L}^{f'} \left(12 \log \frac{M}{m_{f'}} - 9 \right) \pm 3 T_3^{f'} \right\}, \end{split}$$

where M is now the mass of \tilde{S} .

Note that these relations are only valid up to leading order in m_Z/M and $m_{f'}/M$. Nonetheless, in Eqs. (6) and (8), the terms proportional to $m_{f'}^2$ will be much larger than the ones proportional to m_Z^2 when the internal fermion, f', is taken to be the top quark. Thus it will be these terms, proportional to $m_{f'}^2 = m_t^2$, that are particularly constrained by electroweak precision measurements.

The interactions in the RPV Lagrangian in Eq. (2) mimic those of our toy model in Eq. (3). Thus, Eqs. (5)–(8) can also be used to compute the RPV-induced corrections to the $Z\bar{f}f$ couplings. To calculate the modification in the $Z\bar{f}f$ coupling for a fixed final state f, the contributions from all the possible virtual states that can couple to f should be combined. For instance, a nonzero λ'_{332} can modify the $Z\bar{\tau}\tau$ coupling, in addition to the $Z\bar{\nu}_{\tau}\nu_{\tau}$, $Z\bar{b}b$, and $Z\bar{s}s$ couplings. For the final state τ , there can be two combinations of fermions and sfermions in the loop, i.e., t_L -quark and \tilde{s}_R , and s_R -quark and \tilde{t}_L . The contributions from these two virtual states can be calculated using Eqs. (6) and (7) to obtain the correction to the $Z-\tau_L$ interaction:

$$\begin{split} &\Delta g_L^{\tau}(\text{from }\lambda'_{332})\\ &= \frac{3|\lambda'_{332}|^2 m_t^2}{32\pi^2 m_{\tilde{s}_R}^2} \left(2\log\frac{m_{\tilde{s}_R}}{m_t} - 1\right) + \frac{|\lambda'_{332}|^2 m_Z^2}{96\pi^2 m_{\tilde{t}_L}^2} \\ &\quad \times \left\{ \left(-\frac{1}{2} + s_w^2\right) + \left(\frac{1}{3}s_w^2\right) \left(12\log\frac{m_{\tilde{t}_L}}{m_Z} + 1 + \mathbf{i}6\pi\right) \right\}. \end{split}$$

In the above equation, we have ignored a negligible contribution proportional to $m_Z^2/m_{\tilde{s}_R}^2$, arising from the second term of Eq. (6). A similar analysis can be done for any nonzero λ'_{ijk} in any $Z \to f\bar{f}$ channel.

The RPV parameter space is constrained by using Δg^f to predict the Z-pole observables and comparing them with their experimental measurements. The electroweak observables used in this work are shown in Table II, where $\Gamma(\text{inv})$ is the invisible decay width of the Z, $R_\ell \equiv \Gamma(\text{had})/\Gamma(\ell \bar{\ell})$, $R_q \equiv \Gamma(q\bar{q})/\Gamma(\text{had})$, and $A_f \equiv (2g_A^f g_V^f)/((g_A^f)^2 + (g_V^f)^2)$. In these expressions, $\Gamma(\text{had})$ is the partial width of Z into hadrons, and g_V^f and g_A^f are the effective vector and axial couplings of $Z \to f\bar{f}$.

We are also using in this analysis an additional measure of lepton flavor universality that can be extracted from the electroweak data. In particular, we define four observables:

$$V_{\ell e} \equiv g_{\rm V}^{\ell}/g_{\rm V}^{e}, \qquad A_{\ell e} \equiv g_{\rm A}^{\ell}/g_{\rm A}^{e}, \qquad (10)$$

for $\ell=\mu$, τ . The observables $V_{\ell e}$ and $A_{\ell e}$ are measures of lepton flavor universality in the couplings of the Z-boson and should be unity in the SM; they were found to provide strong constraints on new sources of lepton nonuniversality in Ref. [27]. The best fit values for the g_{VA}^{ℓ} are obtained by

TABLE II. The relevant LEP and SLC observables with their SM predictions [26]. The value of A_{τ} corresponds to measurements at LEP using τ -lepton polarization.

Observable	Experimental	Standard model	Pull
$\Gamma(\text{inv})[\text{MeV}]$	499.0 ± 1.5	501.66 ± 0.05	-1.8
R_e	20.804 ± 0.050	20.734 ± 0.010	1.4
R_{μ}	20.785 ± 0.033	20.734 ± 0.010	1.6
$R_{ au}$	20.764 ± 0.045	20.779 ± 0.010	-0.3
R_b	0.21629 ± 0.00066	0.21579 ± 0.00003	0.8
R_c	0.1721 ± 0.0030	0.17221 ± 0.00003	0.0
A_e	0.15138 ± 0.00216	0.1470 ± 0.0004	2.0
A_{μ}	0.142 ± 0.015	0.1470 ± 0.0004	-0.7
$A_{ au}$	0.1439 ± 0.0043	0.1470 ± 0.0004	-0.7
A_b	0.923 ± 0.020	0.9347	-0.6
A_c	0.670 ± 0.027	0.6678 ± 0.0002	0.1
A_s	0.895 ± 0.091	0.9356	-0.4
$g_V^{e^{\mathrm{a}}}$	-0.03817 ± 0.00047		
$g_V^{\mu \; { m a}}$	-0.0367 ± 0.0023		
$g_V^{ au~\mathrm{a}}$	-0.0366 ± 0.0010		
$g_A^{e^{\mathrm{a}}}$	-0.50111 ± 0.00035		
$g_A^{\mu\mathrm{a}}$	-0.50120 ± 0.00054		
$g_A^{ au~\mathrm{a}}$	-0.50204 ± 0.00064		

^aThese observables are only available in the electronic version of the Review of Particle Physics.

the Particle Data Group [26] but published only in the online version of the Review of Particle Physics. For the four ratios, we obtain

$$V_{\mu e} = 0.961 \pm 0.063, \qquad V_{\tau e} = 0.959 \pm 0.029,$$
 (11)

$$A_{\mu e} = 1.0002 \pm 0.0014, \qquad A_{\tau e} = 1.0019 \pm 0.0015,$$
(12)

where we have used the error correlation matrix for the $g_{V,A}^{\ell}$ from Ref. [28] to obtain the quoted errors. We will find that the observable $A_{\tau e}$ provides the strongest current constraint on the λ'_{33k} couplings.

We place 2σ limits on the RPV couplings by calculating changes in each observable at each point in the parameter space of $(m_{\tilde{f}}, \lambda'_{ijk})$. The masses of sfermions, $m_{\tilde{f}}$, are assumed to be degenerate in these calculations. Since the SM prediction for A_e is already 2σ away from the measurements (see Table II), the limits from A_e are obtained at 3σ (otherwise, the whole parameter space for λ'_{13k} is excluded by A_e , as these couplings always worsen the fit). We perform this analysis for each observable independently to find the strongest limit, which is then fit to a straight line for $m_{\tilde{f}} \geq 1$ TeV and quoted in Table I. Note that the limits we mention should not be assumed to be valid for sfermion masses below 1 TeV.

In Table I, the electroweak limits on λ'_{3jk} for all k are given. For the λ'_{33k} coupling, we also show a bound

from the literature. The quoted literature bound is actually an extrapolation of the bound given in the oft-cited Refs. [14,17] and originally derived in Ref. [22]. This outdated bound is usually quoted as $\lambda'_{33k} < 0.45$ for a sfermion mass of 100 GeV, and derived from R_{τ} . Using the same data and predictions as Ref. [22], we reproduced that result but also derived the bound for sfermion masses of 1 TeV. It is this bound that we show in Table I.

Our new bounds in Table I come from $\Gamma(\text{inv})$ for j=1, 2, and from $A_{\tau e}$ for j=3; we find the latter provides a stronger bound than R_{τ} . Note that, as expected, the constraints on λ'_{33k} are much stronger than the others due to the presence of top quarks in the loops. Meanwhile, the strength of the $\Gamma(\text{inv})$ constraint is due, in large part, to the fact that the SM prediction for $\Gamma(\text{inv})$ is already higher than the experimental value by $\sim 1.8\sigma$, and the RPV contribution always makes this discrepancy worse.

It is useful to point out that the limits from $\Gamma(\text{inv})$ are actually the same for all λ'_{ijk} . This is because the RPV-induced $Z \to \nu \bar{\nu}$ process can only have down quarks in the loop [see the Lagrangian of Eq. (2)]. And since $m_{d,s,b} \ll m_Z$, the RPV-induced Δg_L^{ν} is independent of the down-quark generation index (which in this case is both j and k).

Using the procedure outlined here, we obtained the electroweak limits for all the λ'_{ijk} couplings. We find the strongest electroweak constraint on each of the λ'_{ijk} couplings to be as follows:

For
$$i = 1, 2, 3$$
; $j = 1, 2$; $k = 1, 2, 3$:

$$\lambda'_{i1k}, \lambda'_{i2k} < 1.5 \frac{m_{\tilde{f}}}{1 \text{ TeV}} + 0.41 \text{ from } \Gamma(\text{inv}). \quad (13)$$

For
$$i=1;$$
 $j=3;$ $k=1,2,3:$
$$\lambda'_{13k} < 0.51 \frac{m_{\tilde{f}}}{1 \text{ TeV}} + 0.36 \text{ from } A_e \text{ at } 3\sigma. \tag{14}$$

For
$$i = 2$$
; $j = 3$; $k = 1, 2, 3$:
$$\lambda'_{23k} < 0.66 \frac{m_{\tilde{f}}}{1 \text{ TeV}} + 0.42 \text{ from } R_{\mu}. \quad (15)$$

For
$$i = 3$$
; $j = 3$; $k = 1, 2, 3$:

$$\lambda'_{33k} < 0.54 \frac{m_{\tilde{f}}}{1 \text{ TeV}} + 0.38 \text{ from } A_{\tau e}. \tag{16}$$

Here, $m_{\tilde{f}}$ is the mass of sfermions, taken to be degenerate and ≥ 1 TeV. For the λ'_{3jk} couplings, one sees that the monolepton constraint from the LHC is already stronger than that obtained from the electroweak analysis for λ'_{31k} , and that the monolepton constraint is competitive with the electroweak constraint for λ'_{32k} ; in the latter case, the addition of a dilepton channel to the analysis, or simply additional luminosity in the monolepton channel, should

push the LHC DY constraint beyond that of the electroweak analysis.

For i=1, 2, the electroweak constraints are weaker than those we previously obtained from the LHC data in Ref. [2], with two exceptions. These exceptions are as follows: λ'_{132} (a 3σ bound from A_e), which is about 10% stronger than the bound obtained from the DY data, and is even stronger than our projected bound for the high-luminosity LHC; and λ'_{232} (obtained from R_μ), which is a few percent stronger than our current bound, and is similar to the expected bound from the high-luminosity LHC. Therefore, to reiterate, we find that

$$\lambda'_{132} < 0.51 \frac{m_{\tilde{f}}}{1 \text{ TeV}} + 0.36,$$
 (17)

$$\lambda'_{232} < 0.66 \frac{m_{\tilde{f}}}{1 \text{ TeV}} + 0.42 \tag{18}$$

replace the bounds from DY data in Ref. [2] as the strongest currently available bounds on these two couplings.

It has been noted by previous studies that bounds on certain of the λ'_{ijk} derived by demanding that the renormalization group running of those couplings, along with the top quark Yukawa coupling, remain perturbative up to a scale around 10¹⁶ GeV; these "perturbativity" bounds are calculated assuming a minimal low-energy particle content, a "grand desert" and no significant high-scale threshold effects. The resulting bounds on λ'_{ijk} are typically between 1.0 and 1.1 for sfermion masses around 100 GeV and are only slightly weakened for masses between 1 and 10 TeV. In previous analyses [14], the perturbativity bounds were stronger than the experimental bounds for λ'_{221} and λ'_{3jk} (all j, k). However, this analysis shows that, for sfermion masses of 1 TeV, constraints from the LHC outperform the perturbativity constraints for all λ'_{31k} , and that electroweak precision constraints outperform perturbativity constraints for λ'_{33k} ; in our previous paper [2] we also found much stronger constraints from the LHC for λ'_{221} . Therefore, only for the three couplings λ'_{32k} does one find that the perturbativity constraint (namely, $\lambda'_{32k} < 1.1$) remains stronger than the experimental constraints for $m_{\tilde{f}} = 1$ TeV; we do not anticipate this situation changing with additional LHC data without a significant increase in τ tagging efficiency.

Finally, it is noteworthy that the λ'_{3j3} couplings enter into a proposed solution to the present anomaly in the R_D and R_{D^*} branching fractions [29,30], and therefore the constraints derived here can, at least in principle, affect the ability of RPV models to resolve the anomaly. We reproduced the analysis of Ref. [29] using our improved bounds. In that paper, the authors found that RPV SUSY could shift R_D and R_{D^*} by at most 13.0% from their SM values while remaining consistent with all constraints; this shift, when combined with the theoretical and experimental uncertainties allowed for a solution of the R_D anomaly at

 1σ . With our stronger constraints, the maximum shift in $R_{D^{(*)}}$ falls only slightly, to 10.8%, not changing significantly the viability of the model.

V. NEUTRINO MASSES

As pointed out in Refs. [21,31], certain λ' couplings can also generate contributions to neutrino Majorana masses at one loop. These contributions require chirality flips in both the internal fermion and the scalar lines, the former yielding a dependence on quark masses, and the latter a dependence on the left-right squark mixing. In all, one finds

$$\delta m_{\nu_i} \simeq \frac{3\lambda_{ijj}^2}{8\pi^2} \frac{m_{d_j} m_{\tilde{d}_{jLR}}^2}{m_{\tilde{d}_i}^2} = \frac{3\lambda_{ijj}^2}{8\pi^2} \frac{\xi m_{d_j}^2}{m_{\tilde{d}_j}},\tag{19}$$

where i labels the neutrino flavor and $m_{\tilde{d}_{jLR}}^2 = \xi m_{d_j} m_{\tilde{d}_j}$ parametrizes the left-right mixing for the jth down squark. One expects ξ to be no larger than O(1) though in some models it can be much smaller.

Previous compendia of constraints on the λ' couplings have used bounds on the neutrino masses coming from the kinematics of decays with neutrinos in the final state, namely neutron decay (for ν_e), pion decay (ν_μ), and tau decay (ν_τ). The bound from neutron decay is roughly 1 eV (and has recently been improved by KATRIN [32]), while the bounds on ν_μ and ν_τ from pion and tau decay are many orders of magnitude weaker (190 keV and 18 MeV, respectively [26]). Using these limits, one finds very strong bounds on the λ'_{133} coupling and strong (though weaker) bounds on λ'_{122} and λ'_{233} .

However, in light of current experimental data on neutrinos (see Ref. [26] for a review), including measurements of their Δm^2 from oscillations, and of their absolute mass scales, in KATRIN or deduced from cosmology, the previously used bounds on $m_{\nu_{\mu,\tau}}$ are far too conservative unless one wishes to significantly extend the spectrum of the neutrino sector beyond that of the SM. With that in mind, one should quote more realistic bounds on the λ'_{ijj} couplings assuming neutrino masses in the eV or sub-eV mass range. Using Eq. (19), this is straightforward:

$$\lambda'_{i22} < 0.054 \sqrt{\frac{m_{\tilde{s}}}{1 \text{ TeV}} \frac{m_{\nu_i}}{1 \text{ eV}} \frac{1}{\xi}},$$
 (20)

$$\lambda'_{i33} < 0.0012 \sqrt{\frac{m_{\tilde{b}}}{1 \text{ TeV}} \frac{m_{\nu_i}}{1 \text{ eV}} \frac{1}{\xi}}.$$
 (21)

Here ν_i again refers to the interaction state, with i=1,2,3 corresponding to the ν_e, ν_μ, ν_τ states. As such, m_{ν_i} is not a physical mass but appears in the neutrino mass matrix.

These bounds are quite constraining: for $m_{\nu_i} = 1$ eV and $\lambda'_{ijj} = \xi = 1$, these require the s- and b-squarks to be heavier than 340 TeV and 700 PeV, respectively. And because they

weaken only as the square root of the squark masses, they become even more important for large squark masses, compared to other bounds. Only if left-right mixing in the squark sector were highly suppressed (e.g., μ - and A-terms much smaller than squark masses) would collider and other low-energy bounds become the dominant constraint. For example, the next most powerful constraint on λ'_{122} is a bound from charged current universality, $\lambda'_{122} < 0.43(m_{\tilde{s}}/\text{TeV})$, which only competes with the neutrino bound for $\xi \lesssim 0.01$, and then only in a limited mass range.

VI. CONCLUSIONS

In this paper, we have obtained the first limits on the RPV couplings λ'_{3jk} using Drell-Yan $pp \to \tau \nu$ data from the LHC. We find that the current LHC data can be used to derive constraints on five of the nine λ'_{3jk} couplings that are stronger than any previously obtained. We also have reanalyzed the constraints on all the λ'_{ijk} couplings from the precision electroweak data, updating previous bounds in the literature. In particular, we find that the λ'_{331} and λ'_{332} couplings are still best constrained by electroweak data, but those constraints are now roughly 25% stronger than previously reported, most of that improvement coming from using the lepton-flavor-violating observable $A_{\tau e}$. Finally, we have applied more realistic neutrino mass constraints and find extremely strong bounds on the λ'_{322} and λ'_{333} couplings.

By taking the LHC data, the precision electroweak fits, and the neutrino mass limits all into account, we have obtained new, stronger bounds on the λ'_{3jk} RPV couplings that are valid in the TeV mass range. While we do not expect significant improvements to be forthcoming in the electroweak fits, the analysis of di-tau DY data at the LHC could significantly improve some of the bounds given here. And because our LHC-derived bounds come from the exchange of squarks in the *t*-channel, rather than from on-shell pair production, strengthening these bounds does not necessarily require additional center-of-mass energy, but will happen automatically with the additional luminosity one expects in the next phases of the LHC's experimental program.

ACKNOWLEDGMENTS

The authors wish to thank A. de Gouvêa for helpful conversations. This work was partially supported by the National Science Foundation under Grant No. PHY-1820860. The work of M. Q. is partly supported by Spanish MINECO (Grants No. CICYT-FEDER-FPA2014-55613-P and No. FPA2017-88915-P), by the Catalan Government under Grant No. 2017SGR1069, and by Severo Ochoa Excellence Program of MINEICO (Grant No. SEV-2016-0588).

APPENDIX

In this Appendix, we pull together all of the updated limits on the 27 λ'_{ijk} couplings for completeness. The bounds are given in Table III. For each choice of $\{ijk\}$,

the table shows the currently strongest bound on that coupling. We also show the approximate sfermion mass bound (in TeV) one obtains assuming $\lambda'_{ijk} = 1$.

Entries in which the best limits are derived in this paper are indicated with a dagger. Other bounds come from a variety of processes:

- (i) 11k, 121, 21k, 221, 223, 231 are bounded from mono- and dilepton DY scattering into final state electrons and muons, as derived in Ref. [2];
- (ii) 111 has an additional bound from neutrinoless double beta decay $(0\nu\beta\beta)$, but which falls quickly with the mass scale of the SUSY particles (specifically, the selectron and neutralino), taken to be degenerate here at m_{SUSY} [14,31];
- (iii) 122,123 bounds are from charged current universality in β -decay, and 131 is from atomic parity violation (APV), all of which were first derived in Ref. [11] and updated in Refs. [13,14];
- (iv) i22, i33 bounds come from constraints on contributions to neutrino masses, as discussed in Sec. V. The corresponding mass limits assume $\xi = 1$.

One sees from the table that Drell-Yan scattering at the LHC already provides the strongest bounds on 13 of the 27 coupling constants. With additional luminosity, the LHC is capable of obtaining the strongest bounds on at least three additional couplings (i.e., 131, 321, and 323, where the projected bound at a high-luminosity LHC for 131 can be found in Ref. [2]).

TABLE III. Current upper bounds on λ'_{ijk} , the source of each bound, and the excluded sfermion masses assuming the corresponding $\lambda'_{ijk} = 1$.

ijk	Current bound	Source	Sfermion mass limit [TeV]
($0.16 \frac{m_{\bar{d}_R}}{1 \text{ TeV}} + 0.030$	DY monolepton	6.1
[111] {	$0.16\left(\frac{m_{\rm SUSY}}{1~{\rm TeV}}\right)^{5/2}$	0 uetaeta	2.1
112, 113	$0.16 \frac{m_{\bar{d}_R}}{1 \text{ TeV}} + 0.030$	DY monolepton	6.1
($0.34 \frac{m_{\tilde{q}}}{1 \text{ TeV}} + 0.18$	DY dilepton	2.4
[121] {	$0.43 \frac{m_{\tilde{s}_R}}{1 \text{ TeV}}$	CC universality	2.3
123	$0.43 \frac{m_{\tilde{s}_R}}{1 \text{ TeV}}$	CC universality	2.3
131	$0.19 \frac{m_{\tilde{\imath}_L}}{1~{ m TeV}}$	APV	5.3
132	$0.51 \frac{m_{\tilde{q}}}{1 \text{ TeV}} + 0.36$	$A_e(3\sigma)^{\mathrm{a}}$	1.3
211, 212, 213	$0.090 \frac{m_{\tilde{d}_R}}{1 \text{ TeV}} + 0.014$	DY monolepton	11
221	$0.34 \frac{m_{\tilde{q}}}{1 \text{ TeV}} + 0.074$	DY dilepton	2.7
223	$0.44 \frac{m_{\bar{s}_R}}{1 \text{ TeV}} + 0.040$	DY monolepton	2.2
231	$0.34 \frac{m_{\tilde{q}}}{1 \text{ TeV}} + 0.074$	DY dilepton	2.7
232	$0.66 \frac{m_{\tilde{q}}}{1 \text{ TeV}} + 0.42$	$R_{\mu}^{\;\;\mathrm{a}}$	<1
311, 312, 313	$0.20 \frac{m_{\tilde{d}_R^k}}{1~{ m TeV}} + 0.046$	DY monolepton ^a	4.8
321, 323	$1.5 rac{m_{ ilde{d}^k}}{1 ext{ TeV}} + 0.41$	$\Gamma(inv)^a$	<1
331, 332	$0.54 \frac{m_{\tilde{f}}}{1 \text{ TeV}} + 0.38$	$A_{ au e}^{a}$	1.1
122, 222, 322	$0.054\sqrt{rac{m_{ar{s}}}{1~{ m TeV}}rac{m_{ u_i}}{1~{ m eV}}rac{1}{\xi}}$	ν masses	340
133, 233, 333	$0.0012\sqrt{\frac{m_{\tilde{b}}}{1~\text{TeV}}}\frac{m_{\nu_i}}{1~\text{eV}}\frac{1}{\xi}$	ν masses	7×10^5

^aBounds obtained in this work are indicated with a dagger (†). For the 111 and 121 entries, more than one bound compete for masses above 1 TeV. Bounds from neutrino masses are collected at the bottom of the table and updated in this work; the quoted mass limits assume $m_{\nu_i} = 1$ eV and $\xi = 1$.

- [1] For a recent review of the status of LHC searches for supersymmetry See: A. Canepa, Rev. Phys. 4, 100033 (2019).
- [2] S. Bansal, A. Delgado, C. Kolda, and M. Quiros, Phys. Rev. D 99, 093008 (2019).
- [3] N. Raj, Phys. Rev. D 95, 015011 (2017).
- [4] A. Alves, O. J. P. Eboli, G. Grilli Di Cortona, and R. R. Moreira, Phys. Rev. D 99, 095005 (2019).
- [5] S. Bansal, R. M. Capdevilla, A. Delgado, C. Kolda, A. Martin, and N. Raj, Phys. Rev. D 98, 015037 (2018).
- [6] G. Bhattacharyya, D. Choudhury, and K. Sridhar, Phys. Lett. B 349, 118 (1995).
- [7] M. Aaboud *et al.* (ATLAS Collaboration), Phys. Rev. Lett. 120, 161802 (2018).
- [8] A. M. Sirunyan *et al.* (CMS Collaboration), Phys. Lett. B **792**, 107 (2019).
- [9] A. M. Sirunyan *et al.* (CMS Collaboration), Eur. Phys. J. C 78, 708 (2018).
- [10] A. D. Martin, W. J. Stirling, R. S. Thorne, and G. Watt, Eur. Phys. J. C 63, 189 (2009).
- [11] V. D. Barger, G. F. Giudice, and T. Han, Phys. Rev. D 40, 2987 (1989).
- [12] G. Bhattacharyya and D. Choudhury, Mod. Phys. Lett. A 10, 1699 (1995).
- [13] F. Ledroit and G. Sajot, in2p3-00362621, http://hal.in2p3.fr/ in2p3-00362621 (1998).
- [14] B. C. Allanach, A. Dedes, and H. K. Dreiner, Phys. Rev. D 60, 075014 (1999).
- [15] R. Barbier et al., Phys. Rep. 420, 1 (2005).
- [16] M. Chemtob, Prog. Part. Nucl. Phys. 54, 71 (2005).
- [17] D. Dercks, H. Dreiner, M. E. Krauss, T. Opferkuch, and A. Reinert, Eur. Phys. J. C 77, 856 (2017).

- [18] J. K. Mizukoshi, O. J. P. Eboli, and M. C. Gonzalez-Garcia, Nucl. Phys. **B443**, 20 (1995).
- [19] E. Coluccio Leskow, G. D'Ambrosio, A. Crivellin, and D. Müller, Phys. Rev. D 95, 055018 (2017).
- [20] S. Bansal, R. M. Capdevilla, and C. Kolda, Phys. Rev. D 99, 035047 (2019).
- [21] R. M. Godbole, P. Roy, and X. Tata, Nucl. Phys. B401, 67 (1993).
- [22] G. Bhattacharyya, J. R. Ellis, and K. Sridhar, Mod. Phys. Lett. A 10, 1583 (1995).
- [23] J. M. Yang, Eur. Phys. J. C 20, 553 (2001).
- [24] O. Lebedev, W. Loinaz, and T. Takeuchi, Phys. Rev. D 61, 115005 (2000).
- [25] O. Lebedev, W. Loinaz, and T. Takeuchi, Phys. Rev. D 62, 015003 (2000).
- [26] M. Tanabashi *et al.* (Particle Data Group), Phys. Rev. D 98, 030001 (2018).
- [27] F. Feruglio, P. Paradisi, and A. Pattori, J. High Energy Phys. 09 (2017) 061.
- [28] S. Schael *et al.* (ALEPH, DELPHI, L3, OPAL, and SLD Collaborations and LEP Electroweak Working Group, SLD Electroweak Group, and SLD Heavy Flavour Group), Phys. Rep. **427**, 257 (2006).
- [29] W. Altmannshofer, P. S. Bhupal Dev, and A. Soni, Phys. Rev. D 96, 095010 (2017).
- [30] Q. Y. Hu, X. Q. Li, Y. Muramatsu, and Y. D. Yang, Phys. Rev. D 99, 015008 (2019).
- [31] R. N. Mohapatra, Phys. Rev. D 34, 3457 (1986).
- [32] M. Aker *et al.* (KATRIN Collaboration), arXiv:1909 .06048.